ARTICLES

Olfactory pattern classification by discrete neuronal network states

Jörn Niessing[1] & Rainer W. Friedrich[1]

The categorial nature of sensory, cognitive and behavioural acts indicates that the brain classifies neuronal activity patterns into discrete representations. Pattern classification may be achieved by abrupt switching between discrete activity states of neuronal circuits, but few experimental studies have directly tested this. We gradually varied the concentration or molecular identity of odours and optically measured responses across output neurons of the olfactory bulb in zebrafish. Whereas population activity patterns were largely insensitive to changes in odour concentration, morphing of one odour into another resulted in abrupt transitions between odour representations. These transitions were mediated by coordinated response changes among small neuronal ensembles rather than by shifts in the global network state. The olfactory bulb therefore classifies odour-evoked input patterns into many discrete and defined output patterns, as proposed by attractor models. This computation is consistent with perceptual phenomena and may represent a general information processing strategy in the brain.

Neuronal coding strategies have to satisfy conflicting demands. Representations of sensory inputs should be sensitive to small changes in a stimulus but at the same time robust against noise, implying that the brain should discriminate between some neuronal representations but generalize over others. This conflict could be resolved by classifying sensory inputs into discrete patterns of output activity with a defined stability range so that inputs representing similar information converge onto a common output pattern whereas inputs conveying different information become separated (Supplementary Fig. 1). A discretization of neuronal representations could also subserve higher brain functions including perceptual switching, memory formation and recall, and decision making[1–4]. Discrete classification of neuronal activity patterns may be achieved by attractor-like networks that map continuous inputs onto discrete and stable network states (point attractors)[1,2,5–7]. Such models predict that gradual variations in the input ('morphing') result in abrupt transitions between outputs as boundaries between categories are crossed. In the hippocampus, activity patterns across place cells can indeed undergo sudden and global transitions during morphing of the spatial environment (global remapping)[8]. Results of other morphing studies[9–11], however, are less clear and raise the possibility that transitions between neuronal representations are mediated by small ensembles of neurons within a much larger population.

We used zebrafish to examine the classification of odours in the first olfactory processing centre of the vertebrate brain, the olfactory bulb. Structurally similar odours evoke overlapping patterns of sensory activation across the input channels of the olfactory bulb, the glomeruli[12–15], that become decorrelated at the level of the output neurons, the mitral cells[16–21]. Hence, neuronal circuits in the olfactory bulb amplify small differences between representations of similar odours. Glomerular activity patterns also change substantially with odour concentration[12–15,22,23]; however, odours are usually identified as the same stimulus over a broad concentration range[22,24,25]. This perceptual concentration invariance is inconsistent with a general decorrelation of input patterns but could be explained by pattern classification mechanisms (Supplementary Fig. 1). To examine this possibility, we varied the concentration and molecular identity of odours and measured responses of genetically identified mitral cells by temporally deconvolved two-photon calcium imaging (TDCa imaging)[18]. This approach allows for the detection of firing rate changes across large populations of neurons.

Concentration dependence of responses

In an explant of the intact zebrafish brain, we measured mitral cell responses to the amino acid odours Lys ($n = 140$ mitral cells from 4 olfactory bulbs) and Phe ($n = 128$ mitral cells from 7 olfactory bulbs) at five concentrations (10^{-7} M–10^{-3} M) and to a blank. In addition, the stimulus set contained a chemically related control odour (Arg for concentration series of Lys; Trp for concentration series of Phe; 10^{-5} M) to verify that mitral cell activity patterns evoked by similar odours become decorrelated[16–19].

Increasing odour concentration usually reduced response latency and recruited additional mitral cells. Concentration-response functions of individual mitral cells were, however, diverse (Fig. 1a–c and Supplementary Figs 2a–d and 3). Responses of some mitral cells increased with concentration whereas others peaked at intermediate or low concentrations.

To analyse activity across the mitral cell population we combined responses of all mitral cells into matrices (mitral cells × stimuli), one for each time bin. The similarity between activity patterns (column vectors) evoked by different stimuli and at different times was quantified by the Pearson correlation coefficient (Fig. 1d and Supplementary Figs 2e, f and 4). The mean correlation between activity patterns evoked by Lys (10^{-7} M–10^{-5} M) and the control odour Arg (10^{-5} M) decreased significantly during the odour response ($P < 0.001$; regression analysis) from 0.58 ± 0.11 during the early phase (256–512 ms) to 0.30 ± 0.08 during the late phase (2,048–2,304 ms). Moreover, early reference patterns were often only weakly correlated with activity patterns evoked by the same odour at later times and vice versa (Supplementary Figs 2e and 4). Hence, mitral cell activity patterns were reorganized during the initial phase of the odour response and patterns evoked by different odours became decorrelated[16–19].

Activity patterns evoked by different concentrations of the same odour were highly correlated within a concentration range of

[1]Friedrich Miescher Institute for Biomedical Research, Maulbeerstr. 66, CH-4058 Basel, Switzerland.

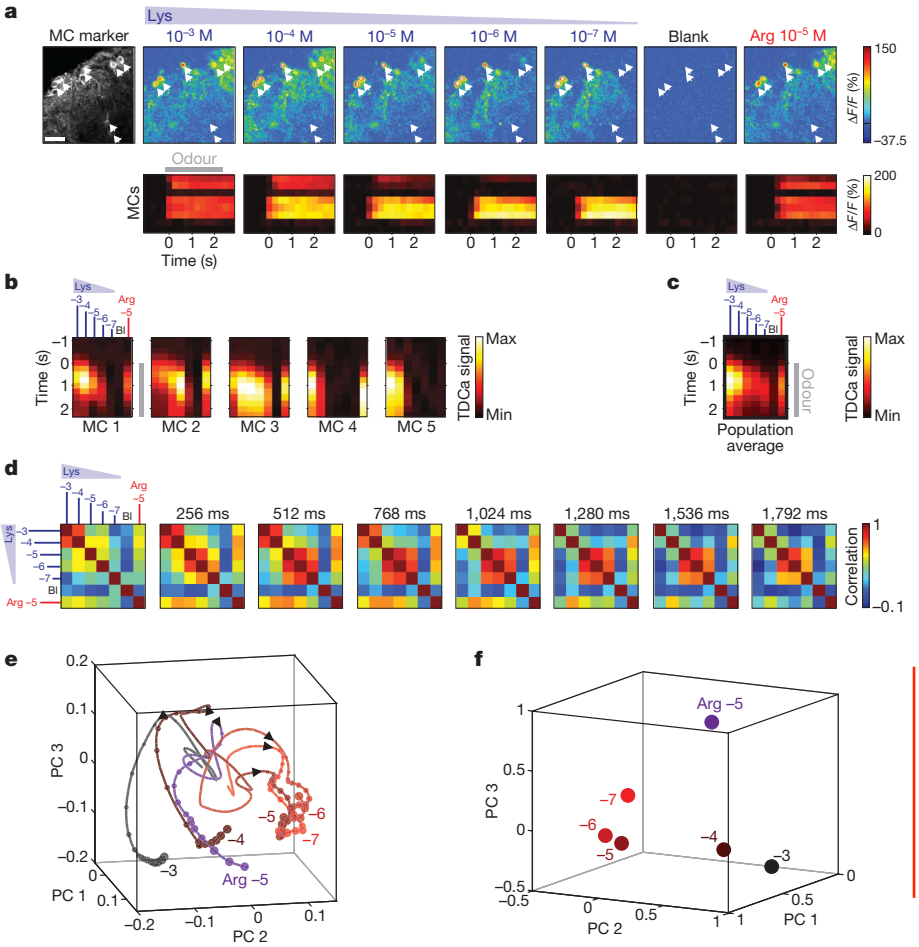

Figure 1 | Concentration dependence of mitral cell odour responses. **a**, Mitral cell (MC) marker expression (left) and raw, time-averaged calcium signals evoked by different concentrations of Lys, a blank (Bl), and the similar control odour Arg. Bottom: raw calcium signals of mitral cells depicted by arrows as a function of time. Scale bar: 25 μm. **b**, Temporally deconvolved calcium signals (TDCa signals) as a function of time, evoked by the same stimuli in five individual mitral cells (different mitral cells than in **a**). Grey bar indicates odour application. **c**, TDCa signals averaged over the population of all recorded mitral cells ($n = 140$ mitral cells from 4 olfactory bulbs). Apparent increases in TDCa signals before response onset ($t = 0$) are mainly due to low-pass filtering of signals (see Methods). **d**, Time series of correlation matrices depicting the pairwise similarity between mitral cell activity patterns evoked by all stimuli in successive time bins. **e**, Representations of odour-evoked activity patterns as a function of time in principal component space (2,048 ms before response onset through to 4,096 ms after response onset). Time is indicated by increasing size of plot symbols (interval: 256 ms). Arrowheads mark response onset and point in the direction of time. **f**, Mitral cell activity patterns in principal component space, time-averaged during the steady state (1,536–2,304 ms).

approximately two to three orders of magnitude (10^{-7} M–10^{-5} M for Lys; Fig. 1d and Supplementary Figs 2e, f and 4). These high correlations were maintained throughout the odour response. The mean correlation between activity patterns evoked by Lys between 10^{-7} M and 10^{-5} M did not significantly decrease ($P > 0.05$, regression analysis). Mean correlations (±s.d.) during the early and late time windows were 0.76 ± 0.10 and 0.67 ± 0.09, respectively. Hence, activity patterns evoked by the same odour within a limited range of concentrations were reorganized, but not decorrelated.

To confirm this result we projected odour-evoked activity patterns onto the first three principal components extracted from time series of activity patterns. Dynamic activity patterns were represented in this three-dimensional space by trajectories that moved from a resting state (spontaneous activity; average over two trials) to a defined subspace representing the steady-state response pattern. Trajectories of Lys at 10^{-4} M and 10^{-3} M and Arg (10^{-5} M) diverged, whereas responses to 10^{-7} M–10^{-5} M Lys converged onto a common subvolume (Fig. 1e, f and Supplementary Movie 1). Similar results were obtained with the concentration series of Phe (Supplementary Fig. 2 and Supplementary Movie 2). Hence, the olfactory bulb did not separate activity patterns evoked by the same odour within a certain concentration range.

Odour morphing

The finding that some inputs to the olfactory bulb are not decorrelated raises the general question how output patterns change when inputs are varied gradually. We therefore morphed one odour (Phe, 10^{-5} M) into a similar odour (Trp, 10^{-5} M) through a series of intermediate mixtures (100/0, 99/1, 90/10, 70/30, 50/50, 30/70, 10/90, 1/99, 0/100). Mitral cell activity patterns evoked by the pure odours were initially highly correlated and subsequently underwent decorrelation[16–19]. Measuring calcium signals from axon terminals of olfactory sensory neurons[12] confirmed that glomerular activation patterns evoked by these stimuli were highly correlated and nearly constant throughout stimulus presentation (Supplementary Fig. 5a, b).

Odour morphing resulted in diverse response changes of individual mitral cells including gradual and abrupt transitions (Fig. 2a, b and Supplementary Figs 3 and 6a, b; $n = 156$ mitral cells in 9 fish), consistent with observations in rats[10]. Analysis of population activity revealed that all mitral cell activity patterns were highly correlated shortly after response onset (Fig. 2c; mean correlation (±s.d.) = 0.78 ± 0.13 at 256 ms). Subsequently, response patterns evoked by the pure components became decorrelated (Fig. 2c, arrows). Patterns evoked by intermediate stimuli did not change gradually but switched abruptly between the 90/10 and 70/30 mixtures from patterns similar to Phe

changed only at one transition point whereas others changed at both, as revealed by templates with single transition points (Fig. 4d, centre and right). Transitions between multiple discrete output patterns are therefore mediated by coordinated response changes among different, yet overlapping, mitral cell ensembles.

Discussion

TDCa imaging of odour responses in zebrafish revealed that mitral cell activity patterns are stable within a range of concentrations but change abruptly during odour morphing. The olfactory bulb therefore classifies sensory inputs into discrete and defined outputs that generalize along some dimensions of coding space (concentration) but make fine discriminations along others (molecular identity).

The diverse concentration-response functions of individual mitral cells indicate that mitral cell activity patterns vary with concentration and contain information about stimulus intensity[20,26,27]. However, unlike patterns evoked by molecularly different odours, mitral cell activity patterns evoked by a range of different odour concentrations were not decorrelated. Odour representations across olfactory bulb output neurons are therefore sensitive to small changes in molecular structure but largely invariant to odour concentration, indicating that mitral cell activity patterns are optimized to represent odour identity rather than intensity. Consistent with this notion, animals can discriminate between closely related molecules but generalize over, or fail to discriminate, different concentrations[22,24,25,28]. Mitral cell activity patterns remained correlated only within a certain concentration range and sometimes changed abruptly when this range was exceeded. It will now be interesting to investigate whether such concentration-dependent pattern changes are related to the recruitment of novel glomerular clusters[12,15] and to sudden changes in odour perception[29,30]. Together, our results suggest that the first processing steps towards the concentration-invariance of odour recognition occur already in the olfactory bulb.

Sudden transitions between mitral cell activity patterns evoked by a morphing series indicate that the coding space encompassing all possible mitral cell activity patterns is discontinuous, consisting of relatively stable regions that are separated by instable transition regions. Hence, neuronal circuits in the olfactory bulb classify glomerular input patterns into discrete and defined outputs (Supplementary Fig. 1). Because pattern transitions are mediated by coordinated response changes among relatively small subsets of mitral cells, discrete output states are clearly defined but not sharply delineated in all dimensions of coding space. Moreover, abrupt pattern transitions are not obvious when mitral cell responses are analysed individually, which is one possible explanation why discrete odour classification has not been detected in responses of mitral cells to morphed odours in rats[10]. Basic properties of neuronal odour classification show interesting parallels to perceptual phenomena. The separation of coding space into discrete stable regions is consistent with perceptual stability against changes in some stimulus variables such as concentration (Supplementary Fig. 1a). The stability of the population response to a 'foreground' odour when another odour ('background') is blended in is consistent with the observation that usually only the foreground odour is perceived (masking)[31–33] (Supplementary Fig. 1b). The separation of binary mixture representations from the representations of both pure components is consistent with the observation that odour mixtures can be perceived as distinct from their components (configural odour perception)[32,34] (Supplementary Fig. 1c). The discrete classification of activity patterns in the olfactory bulb may therefore be reflected, to some extent, in odour perception.

Abrupt transitions between output patterns in response to a gradually changing input are consistent with key predictions of point attractor models. In this context, it should be considered that the steady-state pattern exists only for the duration of the stimulus[7,17,35]. The system is therefore actively 'driven', rather than passively 'attracted', towards an output pattern. Moreover, it is difficult to establish that steady-state activity patterns represent true attractors in the mathematical sense. It remains unclear how our findings relate to attractor models of the olfactory bulb[36] that were developed on the basis of electroencephalogram recordings of oscillatory population activity[37]. In cortical circuits, transitions between output states seem to rely on recurrent excitatory connections[1], whereas interglomerular synaptic pathways in the olfactory bulb are predominantly inhibitory[38] (although excitatory connections between mitral cells occur within glomeruli[39–41]). Our data therefore demonstrate that attractor-like pattern classification can also emerge in circuits dominated by inhibitory interactions.

The discretization of coding space has important consequences for neuronal processing. First, it imposes a limit on the resolution of sensory coding because similar inputs may not become separated even if they are, in principle, distinguishable. A system with high resolving power thus requires a large number of possible output states. Unless the number of neurons is very high, different output patterns may therefore not be orthogonal, consistent with our observations in the olfactory bulb. Second, the classification of inputs into discrete outputs can reduce variations between input patterns such as noise. Pattern classification therefore balances the resolution of sensory representations against noise tolerance. Third, non-isotropic classification can act as a sensory filter by separating input patterns along some stimulus dimensions but generalizing over others (Supplementary Fig. 1). Fourth, the main target area of the olfactory bulb, the pyriform cortex (dorsal posterior telencephalon in zebrafish[42]), has been proposed to function as an autoassociative memory network that performs pattern completion[43,44]. Decorrelated and noise-limited input patterns are prerequisites for this operation. The classification of activity patterns in the olfactory bulb may therefore be an important pre-processing step for cortical computations.

METHODS SUMMARY

Experiments were performed in an explant of the intact nose and brain of adult zebrafish[16]. Mitral cells were identified using a transgenic line expressing a fluorescent marker protein[45]. Bolus loading of olfactory bulb neurons with the red-fluorescing calcium indicator rhod-2-AM (rhod-2 acetoxymethyl ester; Invitrogen R-1245MP) was performed as described[18,19]. The rise time of the stimulus was approximately 600 ms, followed by a plateau of approximately 2 s and a slow decay. Each odour stimulus was repeated twice and responses were averaged. All imaging experiments were performed in the ventro-lateral olfactory bulb that contains most of the amino-acid-responsive mitral cells[42]. In different fish, mitral cell responses were therefore measured from the same region but not necessarily from mitral cells connected to equivalent glomeruli. Calcium signals from mitral cells were measured by multiphoton microscopy[46]. Firing rate changes were reconstructed from the time courses of the calcium signals ($\Delta F/F$) by temporal deconvolution[18]. TDCa signals were then low-pass filtered again using a 1-pole Butterworth filter with a cutoff frequency of 0.2 times the frame rate in both directions. This additional filtering step further increased the accuracy of firing rate reconstructions in each time bin but slightly broadened the time course of signals. TDCa signals were normalized to the maximum of the average mitral cell responses in each experiment and pooled over experiments. Additional controls are shown in Supplementary Figs 10 and 11. Calcium signals from afferent axon terminals were measured in the same region as mitral cell responses by selective loading of a calcium indicator into olfactory sensory neurons as described[12]. Calcium signals from glomerular afferents were not temporally deconvolved because the raw calcium signal is directly related to transmitter release[47,48]. Statistical comparisons were performed using a non-parametric Mann–Whitney *U*-test.

Full Methods and any associated references are available in the online version of the paper at www.nature.com/nature.

Received 27 July 2009; accepted 24 February 2010.
Published online 14 April 2010.

1. Wang, X. J. Decision making in recurrent neuronal circuits. *Neuron* **60**, 215–234 (2008).
2. Machens, C. K., Romo, R. & Brody, C. D. Flexible control of mutual inhibition: a neural model of two-interval discrimination. *Science* **307**, 1121–1124 (2005).
3. Leopold, D. A. & Logothetis, N. K. Multistable phenomena: changing views in perception. *Trends Cogn. Sci.* **3**, 254–264 (1999).

METHODS

Animals, dye loading and odour stimulation. Experiments were performed in 38 adult zebrafish (*Danio rerio*; >3 month old). All animal procedures were performed in accordance with official animal care guidelines and approved by the Veterinary Department of the Canton of Basel-Stadt (Switzerland). Mitral cells were identified using a transgenic line (HuC-YC)[49] that in the olfactory bulb expresses the yellow fluorescent marker protein, yellow cameleon 2.1 (YC)[50], selectively in mitral cells[45]. Briefly, fish were anaesthetized on ice, decapitated and olfactory bulbs were exposed by removal of the eyes, jaws and bones over the ventral telencephalon. The resulting explant preparation of the intact brain and nose was then superfused continuously with oxygenized Ringer solution containing 124 mM NaCl, 10 mM glucose, 2 mM KCl, 1.6 mM $MgSO_4$, 2 mM $CaCl_2$, 1.25 mM KH_2PO_4, 24 mM $NaHCO_3$, 25 mM HEPES, 15 mM NaGluconate and 9 mM NaOH and warmed up to room temperature (~23 °C). This solution was similar to teleost artificial cerebrospinal fluid[51] but contained HEPES instead of carbonate for pH buffering.

Bolus loading of olfactory bulb neurons with the red-fluorescing calcium indicator rhod-2-AM was performed as described[18,19]. Measurements started 30–60 min after termination of the dye loading procedure. Amino acid odours were of the highest available purity (≥99.0%, Fluka) and applied through a flow directed at the ipsilateral naris using a computer-controlled, pneumatically actuated HPLC injection valve (Rheodyne). Amino acids are natural odours for zebrafish with response thresholds in the nanomolar range and maximal concentrations within food sources in the millimolar range[52,53]. The concentration range in our experiments is therefore assumed to cover most of the physiological range[52,53]. Stimuli were delivered in a pseudo-random sequence to minimize possible hysteresis effects and separated by at least 90 s to avoid adaptation.

Temporally deconvolved calcium imaging of mitral cell activity. Odour-evoked calcium signals were measured in the ventro-lateral part of the olfactory bulb by two-photon microscopy[46]. Within a given focal plane, raw calcium signals from mitral cells were initially measured in response to the odour at 10^{-5} M (concentration experiments), to the 50/50 mixture, or to the pure odours (morphing experiments). If none of the mitral cells responded to these odours, a new focal plane was selected. If a focal plane clearly contained responsive mitral cells, responses of all mitral cells in this plane were included in the data set. This procedure reduces the number of non-responsive mitral cells in the data set but should have only minimal consequences on the results because non-responsive neurons do not change the general outcome of the analyses. In each fish, usually 3–4 focal planes were examined.

Odour-evoked calcium signals in mitral cells were measured using a custom-built two-photon fluorescence microscope equipped with a mode-locked Ti:sapphire laser (SpectraPhysics) and a 20× objective (NA 1.0, Zeiss). Yellow (YC) and red (rhod-2) fluorescence emission was detected by an external photomultiplier-based whole-field detector through emission filters (515/30 and 610/75 nm). Laser intensity was adjusted in each focal plane to minimize photobleaching. Images were acquired at 256 ms per frame in concentration experiments and 128 ms per frame in morphing experiments using SCANIMAGE software (http://svobodalab.cshl.edu/)[54].

Series of fluorescence images were averaged across trial repetitions and converted into image series depicting the relative change in fluorescence ($\Delta F/F$) in each pixel. Baseline fluorescence was calculated by averaging the raw pixel values over at least 1 s before onset of the odour stimulus. Time-averaged maps of calcium signals were calculated by averaging the $\Delta F/F$ images over a period of approximately 3 s after activity onset and spatially filtered with a mild Gaussian kernel (five pixels). All colour scales are linear. Mitral cell somata were identified in images of YC fluorescence and outlined manually. Firing rate changes were reconstructed from the time course of the calcium signal in each mitral cell by temporal deconvolution as described[18]. Parameters used for deconvolution[18] were $\tau_{decay} = 3$ s and $thr_{noise} = 1\%$ as determined previously[18]. TDCa signals were then low-pass filtered again using a 1-pole Butterworth filter with a cutoff frequency of 0.2 times the frame rate in both directions. This additional filtering step increased the accuracy of firing rate reconstructions, as found by a direct comparison between TDCa signals and simultaneously measured action potentials. It also slightly broadened the time course, which accounts for the apparent increase of the TDCa signal before stimulus onset in some cases.

Calcium imaging of glomerular activation patterns. Calcium signals from afferent axon terminals were measured after loading of Oregon Green 488 BAPTA-1-dextran (OGB1-dextran; 10 kDa; Invitrogen) into olfactory sensory neurons as described[12]. Signals were measured in the same region as mitral cell responses (ventro-lateral olfactory bulb). Briefly, fish were anaesthetized in 0.01% tricaine methanesulphonate (MS-222) and a solution of 2–5% OGB1-dextran was infused into the noses for 5 min. After 3–6 days, odour-evoked calcium signals were measured in the explant preparation using epifluorescence optics (objective: 20×; NA 1.0; Zeiss) and a sensitive CCD camera (CoolSnap; Photometrics). Calcium signals were normalized as data from mitral cells and assigned to glomeruli as described[12].

Data analysis. Data analysis was performed using routines written in IgorPro (Wavemetrics) and MATLAB (The Mathworks). For some analyses, data acquired at 128 ms per frame were down-sampled to 256 ms per frame by averaging successive frames. Before the second low-pass filtering step, TDCa signals were normalized to the maximum of the average mitral cell responses in each experiment. Because the delay between valve switching and stimulus arrival varied slightly between experiments, TDCa signals were aligned in time on the onset of the population response. After temporal alignment, data from different experiments were pooled. Time $t = 0$ was assigned to the onset of the mean activity in the pooled data set by finding the time when the mean activity started to deviate from baseline. Because it is sometimes difficult to unambiguously define this time point we tested different methods (manual detection, different fixed thresholds, different thresholds based on the s.d.) and found that the time defined as $t = 0$ varied maximally by 256 ms, usually less. Pooled response matrices were then low-pass filtered (see above), which smeared out the TDCa signals in time over a period of at least 384 ms. Hence, the potential imprecision in determining $t = 0$ is relatively small compared to the effect of low-pass filtering. The broadening of TDCa signals by low-pass filtering should be considered in the interpretation of response time courses.

Mitral cells were counted as responsive in a given time bin when the TDCa signal exceeded two times the s.d. of the TDCa signal from the same cell in the absence of odour stimulation. The s.d. was calculated from 10-s measurements without odour stimulation in separate trials.

To compute trajectories in principal component space, matrices containing cells as rows and stimuli as columns at each time bin were appended column-wise, resulting in one matrix containing all cells as rows and all stimuli in consecutive time bins as columns (number of columns = stimuli × time bins). Principal components were then extracted after standardizing columns to obtain one coefficient for each stimulus–time bin pair on each principal component. Principal components are orthogonal basis vectors representing the variance in the original data set in decreasing order. The coefficients of each odour on the first three principal components therefore visualize odour-evoked activity patterns in an orthogonal three-dimensional space that retains the maximum possible variance in the data. For plots of trajectories, data points were interpolated between time bins. Principal component analysis on patterns in the steady state was performed using the same procedure on time-averaged activity patterns (number of time bins = 1).

To confirm the robustness of results from correlation and principal component analysis, analyses were performed repeatedly (10 times) after randomly eliminating 50% of mitral cells in each data set. Similar results were obtained with different subsets of mitral cells, demonstrating that results were not critically biased by small sampling size (Supplementary Fig. 10). Correlations between patterns of spontaneous calcium signals or between shuffled activity patterns were near zero (Supplementary Fig. 11). In concentration experiments in individual fish, persistent clusters of patterns that did not undergo decorrelation were observed in each fish but the boundaries were variable. This may be due to the limited number of mitral cells recorded in each fish (24 ± 16 mitral cells per fish; mean ± s.d.) or reflect inter-individual variability. In morphing experiments, sharp transitions between activity patterns at similar positions in the morphing series were observed in data sets from a subset of individuals (Supplementary Fig. 8), consistent with the finding that transitions are mediated by small subsets of mitral cells. In an additional set of experiments ($n = 99$ mitral cells from 5 fish), we morphed one odour (Trp) into a second, similar odour (Tyr) and then morphed the second odour (Tyr) into a more dissimilar odour (Ala). We again observed one transition during morphing of the similar odours (Trp/Tyr) and two transitions during morphing of the dissimilar odours (Tyr/Ala) (data not shown).

Calcium signals measured in glomerular afferents after loading of OGB1-dextran were not temporally deconvolved. In rodents, transmitter release from axons of olfactory sensory neurons depends almost linearly on the intracellular calcium concentration[47] and raw calcium signals are highly correlated to transmitter release[48]. The time course of the raw calcium signal is therefore likely to be a good estimator for transmitter release and, thus, synaptic input to olfactory bulb neurons. Nevertheless, we also determined the time constant of calcium transients in axon terminals of sensory neurons by measuring calcium transients in response to electrical stimulation of the olfactory nerve. We found the dominant time constant to be very short (~100 ms) compared to the time constant of calcium transients in mitral cell somata (~3 s). Deconvolving calcium signals from glomerular afferents with this time constant changed the time course of signals only minimally. As a consequence, the effect on correlations was negligible.

To sort transitions between mitral cell responses into different categories (Supplementary Fig. 3), responses of each mitral cell to series of different concentrations or mixture ratios were fit by linear, quadratic and sigmoid functions[10,11]. For each fit, the variance explained by the fit relative to the non-explained variance (F statistic) was calculated, which takes into account the different degrees of freedom for the different functions. To calculate the variance, the mean was not subtracted to